

## Evidence for a Calcium-Sensing Receptor in the Vascular Smooth Muscle Cells of the Spiral Modiolar Artery

K. Wonneberger<sup>1,2</sup>, M.A. Scofield<sup>3</sup>, P. Wangemann<sup>1</sup>

<sup>1</sup>Cell Physiology Laboratory, Kansas State University, Manhattan, KS 66506, USA

<sup>2</sup>Dept. Otolaryngology at Unfallkrankenhaus Berlin, Berlin, Germany

<sup>3</sup>Pharmacology Department, Creighton University, Omaha, NE, USA

Received: 1 December 1999/Revised: 9 March 2000

**Abstract.** The vascular diameter of the gerbilline spiral modiolar artery has been shown to depend on the presence of extracellular  $\text{Ca}^{2+}$  but it remained unknown whether the smooth muscle cells of this arteriole contain a  $\text{Ca}^{2+}$  sensing receptor (CaSR). The cytosolic  $\text{Ca}^{2+}$  concentration ( $[\text{Ca}^{2+}]_i$ ) was monitored as fluo 3 fluorescence and the vascular diameter was measured by video-microscopy in isolated in vitro superfused spiral modiolar arteries. RT-PCR was used to probe for the presence of CaSR transcripts. Increasing the extracellular  $\text{Ca}^{2+}$  concentration ( $[\text{Ca}^{2+}]_o$ ) from 1 to 10 mM caused a biphasic increase in  $[\text{Ca}^{2+}]_i$  that was paralleled by a vasoconstriction. The initial rate of this vasoconstriction,  $2.01 \pm 0.07 \mu\text{m}/\text{sec}$  ( $n = 131$ ), was inhibited when cytosolic  $\text{Ca}^{2+}$  stores were presumably depleted with thapsigargin ( $IC_{50} = 3 \times 10^{-9} \text{ M}$ ,  $n = 26$ ) or ryanodine ( $IC_{50} = 4 \times 10^{-8} \text{ M}$ ,  $n = 25$ ) or when PLC was inhibited by  $10^{-6} \text{ M}$  U73122 ( $n = 8$ ). The initial rate of this constriction was not affected by the L-type  $\text{Ca}^{2+}$  channel blocker  $10^{-6} \text{ M}$  nifedipine ( $n = 5$ ), by  $10^{-6} \text{ M}$  U73343 ( $n = 6$ ), which is the inactive analogue of U73122, by the T-type  $\text{Ca}^{2+}$  channel blocker  $10^{-6} \text{ M}$   $\text{Gd}^{3+}$  ( $n = 6$ ) or the  $\text{Na}^+/\text{Ca}^{2+}$  exchanger blocker  $10^{-4} \text{ M}$   $\text{Ni}^{2+}$  ( $n = 5$ ). The agonist rank potency order was  $\text{Gd}^{3+} > \text{Ni}^{2+} > \text{Ca}^{2+} \gg \text{neomycin} = \text{Mg}^{2+}$ . Analysis of RNA isolated from the SMA revealed a RT-PCR product of the appropriate size for the CaSR (448 bp). Sequence analysis of the amplified cDNA fragment revealed a 94–96% amino acid identity compared to other CaSRs. These results demonstrate that the spiral modiolar artery contains a CaSR, which is most likely located in the vascular smooth muscle cells.

**Key words:** Calcium-sensing receptor — Cerebral arter-

ies — Labyrinth — Thapsigargin — Ryanodine — U73122

### Introduction

The spiral modiolar artery originates via the anterior inferior cerebellar artery from the basilar artery and provides the main blood supply to the cochlea. This vessel is of great interest since alterations of blood flow along this arteriole are thought to be involved in the pathogenesis of hearing loss and tinnitus. In general, blood flow is related to the vascular diameter according to the law of Hagen-Poiseuille and the vascular diameter depends on the contractile state of the vascular smooth muscle cells (VSMC).  $\text{Ca}^{2+}$  plays a key role in the contractility of vascular smooth muscle cells. Indeed, it has been demonstrated that small increases in the intracellular  $\text{Ca}^{2+}$  concentration ( $[\text{Ca}^{2+}]_i$ ) cause already substantial contractions of vascular smooth muscle cells (Morgan, 1987). In contrast, changes of the extracellular  $\text{Ca}^{2+}$  concentration ( $[\text{Ca}^{2+}]_o$ ) have been shown to have various effects on the vascular diameter of different arteries. Some arteries constrict, when  $[\text{Ca}^{2+}]_o$  is elevated, whereas others dilate or appear to be relatively insensitive to changes in  $[\text{Ca}^{2+}]_o$  (Uchida & Bohr, 1969; Altura & Altura, 1978; Webb & Bohr, 1978; Ito et al., 1991; Wylam et al., 1993; Bukoski et al., 1997; Noguera et al., 1998). In a previous study, we have shown that the vascular tone of the spiral modiolar artery depends on the presence of  $[\text{Ca}^{2+}]_o$ . Isolated vessel segments lose their tone when exposed to a nominally  $\text{Ca}^{2+}$ -free medium (Wangemann et al., 1998). This finding raises the question whether the spiral modiolar artery responds to elevations of  $[\text{Ca}^{2+}]_o$  and possesses the ability to sense  $[\text{Ca}^{2+}]_o$  via a  $\text{Ca}^{2+}$ -sensing receptor (CaSR).

Tissues such as parathyroid, thyroid, kidney and bone, that recognize and regulate the systemic  $\text{Ca}^{2+}$  homeostasis, have been shown to sense  $[\text{Ca}^{2+}]_o$  via CaSR (Brown et al., 1993; Zaidi et al., 1993; Riccardi et al., 1995; McGehee et al., 1997).

Recently, CaSRs have also been found in tissues which are not known to be involved in the systemic  $\text{Ca}^{2+}$  homeostasis. These tissues include the central and peripheral nervous system, lens and ovary epithelial cells. In these tissues,  $[\text{Ca}^{2+}]_o$  via the CaSR is thought to modulate functions such as neurotransmitter release, intracellular ion homeostasis, cellular proliferation and differentiation (Ruat et al., 1995; Bukoski et al., 1997; Chattopadhyay et al., 1997; McNeil et al., 1998).

Agonist-induced activation of the CaSR causes an increase in  $[\text{Ca}^{2+}]_i$  that arises from two distinct mechanisms: (a) mobilization of  $\text{Ca}^{2+}$  from intracellular stores, i.e., the endoplasmic reticulum, and (b) influx of extracellular  $\text{Ca}^{2+}$  through voltage-insensitive channels (Nemeth, 1995). Most CaSRs have been shown to be linked to a G protein-mediated second messenger pathway, which activates phospholipase C (PLC) (Brown et al., 1993; Ruat et al., 1996; McNeil et al., 1998). PLC hydrolyzes phosphatidylinositol 4,5-bisphosphate to inositol(1,4,5)-triphosphate ( $\text{IP}_3$ ) and diacylglycerol (DAG).  $\text{IP}_3$  mobilizes stored  $\text{Ca}^{2+}$  from the endoplasmic reticulum, resulting in fast increases in  $[\text{Ca}^{2+}]_i$  and DAG activates protein kinase C (Berridge, 1993). The fast increase in  $[\text{Ca}^{2+}]_i$  triggers an influx of  $\text{Ca}^{2+}$  across the plasma membrane in accordance with the capacitative calcium influx model (Putney & McKay, 1999).

Evidence for the presence of a CaSR can be obtained using functional and molecular biological assays. A functional demonstration of the CaSR may include a demonstration (a) that an elevation of  $[\text{Ca}^{2+}]_o$  causes an elevation of  $[\text{Ca}^{2+}]_i$ , (b) that the  $[\text{Ca}^{2+}]_o$ -induced increase in  $[\text{Ca}^{2+}]_i$  involves release of  $\text{Ca}^{2+}$  from cytosolic stores, (c) that the  $[\text{Ca}^{2+}]_o$ -induced increase in  $[\text{Ca}^{2+}]_i$  does not occur via voltage-sensitive  $\text{Ca}^{2+}$  channels, (d) that  $\text{Gd}^{3+}$  and  $\text{Ca}^{2+}$  are agonists and (e) that CaSR transcripts are present.

The aim of the present study was to determine whether the spiral modiolar artery contains a CaSR, which will allow this arteriole to respond to changes in  $[\text{Ca}^{2+}]_o$ . Parts of this study have been presented at recent meetings (Wonneberger & Wangemann, 1999; Wonneberger et al., 2000).

## Materials and Methods

### PREPARATION

Experiments were conducted on tissues isolated from gerbils. Gerbils were anesthetized with sodium pentobarbital (100 mg/kg i.p.) and decapitated under a protocol approved by the Institutional Animal Care

and Use Committee at Kansas State University. The spiral modiolar artery was isolated from the cochlea by microdissection and used in functional and molecular biologic studies. In addition, gerbil kidneys were obtained for molecular biologic studies (*see below*). The dissection of the spiral modiolar artery has been described previously (Wangemann & Gruber, 1998). Briefly, the temporal bones were removed from the head, opened and placed into a microdissection chamber maintained at 4°C. The otic capsule enclosing the cochlea was opened and the spiral modiolar artery was visualized through the very thin bone surrounding the modiolus. The bone surrounding the modiolus was then carefully removed and the spiral modiolar artery, which is only loosely attached to the eighth cranial nerve, was isolated. Care was taken to not excessively stretch the artery.

### FUNCTIONAL STUDIES

A 250 to 350  $\mu\text{m}$  segment was cut from the isolated spiral modiolar artery and transferred into a bath chamber mounted on the stage of an inverted microscope (TE 300 or Diaphot, Nikon, Japan). In the bath chamber, the vessel was held in place with two blunted glass needles mounted on micromanipulators (Narashige, Japan). The mounted vessel was superfused at a rate of 2.5 times the bath chamber volume per second. All experiments were performed at 37°C. The control superfusate contained (in mM): 150 NaCl, 5.0 HEPES, 3.6 KCl, 1  $\text{MgCl}_2$ , 1  $\text{CaCl}_2$  and 5.0 glucose, pH 7.4. In some experiments the  $\text{K}^+$  concentration was elevated to 150 mM by substituting KCl for NaCl. Drugs were added to these solutions as appropriate. Thapsigargin (Sigma, St. Louis, MO), ryanodine (Sigma), U73122 (RBI, Natick, MA) and U73343 (RBI) were predissolved in DMSO. The final concentration of DMSO was 0.05%.  $\text{Ca}^{2+}$  or  $\text{Mg}^{2+}$  concentrations were increased by adding  $\text{CaCl}_2$  or  $\text{MgCl}_2$  and  $\text{Ni}^{2+}$  or  $\text{Gd}^{3+}$  were introduced by adding  $\text{NiCl}_2$  or  $\text{GdCl}_3$ .

### MEASUREMENT OF THE VASCULAR DIAMETER

Videomicroscopy was used to monitor the vascular diameter as described earlier (Wangemann & Gruber, 1998). The inverted microscope was equipped with a black and white video camera (WV-1410, Panasonic). The microscope image was mixed with a time signal (Time Code Generator, Fast Forward Video, Irvine, CA) and was displayed on a monitor (PVM-122, Sony) as well as recorded on videotape (AG-1960, Panasonic). The outer diameter of the spiral modiolar artery was monitored by two video-edge detectors (Crescent Electronics, East Sandy, UT). The calibrated distance between the two tracked edges was monitored online with a chart-recorder as well as digitized at a frequency of 12 Hz. The digitized data were stored in ASCII format by an acquisition program written in a programmable data analysis and plotting program (Origin 4.1, Microcal Software, Northampton, MA). The resolution of the video microscopy system was 0.12  $\mu\text{m}$  and 0.08 sec.

### MEASUREMENT OF INTRACELLULAR $\text{Ca}^{2+}$ $[\text{Ca}^{2+}]_i$

Microfluorometry was used to monitor  $[\text{Ca}^{2+}]_i$ . Segments of the spiral modiolar artery were incubated for 30 min with 5  $\mu\text{M}$  fluo-3-AM at room temperature (22°C) to load the cells with the  $\text{Ca}^{2+}$ -indicator dye fluo-3 (Molecular probes, Eugene, Oregon). Subsequently the tissue was mounted in the superfusion chamber on the stage of the inverted microscope. The preparation was alternately (100 Hz) illuminated with light of 440 and 488 nm (Deltascan, Photon Technology International, South Brunswick, NJ). The emitted fluorescence limited with a band-pass filter to a wavelength of  $526 \pm 12$  nm was detected with a photon-

counter (Photon Technology International) at a rate of 1 Hz. Changes in the emission intensity in response to excitation with 488 nm light were taken as a measure of changes in  $[Ca^{2+}]_i$ , although changes in the fluorescent dye concentration could not be ruled out. A much smaller signal was detected in response to excitation with 440 nm light. This signal, however, was too small in magnitude to be used as an indicator for changes in dye concentration.

To detect changes in dye concentration a second fluorescent dye was loaded. Putative changes in dye concentration would be detected in the same tissue sample subsequent to the detection of changes in  $[Ca^{2+}]_i$ . Thus, fluo-3 loaded spiral modiolar artery segments mounted in the bath chamber on stage of the inverted microscope were incubated with 1  $\mu$ M BCECF-AM (Molecular Probes, Eugene, Oregon) for about 1 min at room temperature to load the fluorescent dye BCECF. Loading was monitored to achieve an emission intensity in response to 440 nm excitation light that was similar in magnitude to the emission intensity emitted from fluo 3 in response to 488 nm excitation light. Changes in the fluorescence intensity emitted in response to excitation with 440 nm light were taken as a measure of changes in dye concentration since BCECF has an isosbestic point at this excitation wavelength. Viability of the double-loaded spiral modiolar artery segments was verified by measuring the vascular diameter as described above and performing maneuvers known to cause vasoconstriction, *see* Results.

## PHARMACOLOGIC ANALYSIS

Agonist-induced vasoconstrictions were compared by quantifying the size of their initial rate and the magnitude of the plateau reached at the end of the stimulus (Fig. 1). Data obtained in one vessel segment were normalized to  $[Ca^{2+}]_o$ -induced vasoconstrictions performed at the beginning of the experiment. The concentration of a drug that caused a half-maximal inhibition of the  $[Ca^{2+}]_o$ -induced vasoconstriction was obtained by nonlinear curve fit to the equation

$$E = E_{Ins} + \frac{E_{max} \times (1 - C^h)}{IC_{50}^h + C^h}$$

where  $E$  is the relative effect (%),  $E_{max}$  is the maximal effect,  $E_{Ins}$  is the inhibitor-insensitive component of the effect,  $C$  is the concentration of inhibitor and  $h$  defines the slope.

## MOLECULAR BIOLOGICAL STUDIES

Total RNA was extracted from samples of gerbil kidney and gerbil spiral modiolar artery. Kidneys were isolated and immediately placed into liquid nitrogen, pulverized with a mortar and pestle, and transferred into TRIzol reagent (GIBCO BRL, Life Technologies), a monophasic solution of phenol and guanidine isothiocyanate. Spiral modiolar arteries were isolated by microdissection within 7 min (first ear) and 15 min (second ear) of the sacrifice of each animal and directly transferred from the 4°C dissection medium into TRIzol reagent. Spiral modiolar arteries from 8 ears were pooled in the TRIzol reagent. Vessels were homogenized in the TRIzol reagent and the total RNA was extracted according to the manufacturer's procedure. Total RNA was precipitated by isopropanol and dissolved in RNase-free water (diethylpyrocarbonate treated water). The nucleic acid concentration was determined spectrophotometrically. RNA samples were stored at -70°C. Before analysis of the RNA samples by reverse-transcription polymerase chain reaction (RT-PCR), DNA contamination was removed by treatment with amplification-grade RNase-free DNase I (GIBCO BRL, Life Technologies) for 15 min at room temperature.

DNase I was consequently deactivated by heat treatment according to the manufacturer's protocol.

## CDNA SYNTHESIS AND PCR AMPLIFICATION

Sense and antisense gene-specific primers for the CaSR were designed based on sequence information for the rat CaSR (accession #U20289, GenBank/EMBL database), murine CaSR (#AF110179), bovine CaSR (#S67307) and human CaSR (#NM000388). The primers targeted a region of 137 amino acids in exon 6, which spans from the interface between the putative TM5 segment and the third cytoplasmic loop (sense primer) into the putative cytoplasmic tail (antisense primer). According to the rat sequence (#U20289), the sense primer was located at nucleotide 2553-2573 with a sequence of 5'-CCATCT-GCTTCTTCTTGCC-3'. A degenerate primer was used as the antisense primer and was based on a consensus of rat, bovine, murine and human CaSR sequences. The location of the antisense primer with respect to the rat sequence (#U20289) was 2982-3000 with a sequence of 5'-TGCTG(C/T)TGCTTCTGCTCTC-3'. The expected size of the RT-PCR product was 448 bp.

DNase-treated total RNA was reverse transcribed into cDNA in a 10  $\mu$ l reaction. The reaction contained 0.1–1.0  $\mu$ g total RNA, 10 units RNasin (Promega), 1 mM dNTP (GIBCO BRL, Life Technologies), 5 units Moloney Murine Leukemia Virus Reverse Transcriptase (Perkin-Elmer), 5.0 mM  $MgCl_2$  (GIBCO BRL, Life Technologies), 2.5  $\mu$ mol random hexamers (Perkin-Elmer), 20 mM Tris-HCl and 50 mM KCl. Tris-HCl and KCl were added from a 10X PCR buffer (GIBCO BRL, Life Technologies). The RT reaction was incubated at 42°C for 50 min, 5 min at 99°C, and 5 min at 5°C (Perkin-Elmer 480 DNA Thermal Cycler).

PCR was performed in a 50  $\mu$ l reaction. This reaction contained the 10  $\mu$ l RT reaction mix, 25 pmol of the antisense and the sense primer and 1.25 units Taq DNA polymerase (GIBCO BRL, Life Technologies). The final concentrations of  $MgCl_2$ , KCl and Tris-HCl were adjusted to 3.0 mM, 50 mM and 20 mM, respectively. The PCR reaction mix was incubated as follows: 1 denaturation cycle for 5 min at 95°C; 40 amplification cycles consisting of: denaturation for 1 min at 95°C, annealing for 1 min at 58°C and extension for 1 min at 72°C; and one extension cycle for 5 min at 72°C. PCR products were analyzed by horizontal electrophoresis on a 2% agarose gel, stained with ethidium bromide, and documented (BIO-RAD 1000 gel documentation system).

## CLONING AND SEQUENCING OF AMPLIFIED CDNA FRAGMENTS

Amplified cDNA fragments were excised from a low-melt agarose gel (FMC, BioProducts) and cloned into a pCR@2.1 vector with a TA cloning® kit (Invitrogen). Recombinant plasmids were isolated from the colonies using the standard alkaline lysis procedure, purified by phenol/chloroform extraction, and precipitated and washed with ethanol. Insertion of the PCR product into the plasmid was confirmed by restriction endonuclease digestion with *Eco*RI and subsequent horizontal gel electrophoresis. The recombinant double stranded plasmid served as a template for cycle sequencing using M13 forward and reverse primers and fluorescence-based dideoxy nucleotides (PRISM Ready Reaction Dye Deoxy Terminator Cycle Sequencing Kit, Perkin Elmer). The sequence was determined using a DNA Sequencer (ABI Model 373, Applied Biosystems). The sequence was validated by sequencing RT-PCR products from three separate RT-PCR reactions. The identity of the obtained sequence was determined by comparison to known sequences (FastA, Wisconsin Package, Genetics Computer Group; GenBank/EMBL).

## STATISTICS

Data are presented as mean and SE. The number of experiments ( $n$ ) represents the number of vessel segments. Statistical analysis involved paired  $t$ -tests to compare data obtained in paired experiments and analyses of variance when appropriate.

## Results

The present study is based on data from 141 isolated superfused vessel segments which had an outer diameter of  $63 \pm 1 \mu\text{m}$ . Tissues, which are known to contain a CaSR, respond to an elevation of the  $[\text{Ca}^{2+}]_o$  with an increase in  $[\text{Ca}^{2+}]_i$ . Therefore, in a first series of experiments, the effect of an elevation of  $[\text{Ca}^{2+}]_o$  on  $[\text{Ca}^{2+}]_i$  was determined using the fluorescent dye fluo-3. Elevation of  $[\text{Ca}^{2+}]_o$  from 1 to 10 mM evoked a biphasic increase in fluo-3 fluorescence intensity (Fig. 1A) but had no significant effect on BCECF fluorescence (*data not shown*). These observations demonstrate that the observed increase in fluo-3 fluorescence was due to an increase in  $[\text{Ca}^{2+}]_i$  rather than merely a change in the dye concentration. The increase in  $[\text{Ca}^{2+}]_i$  induced by an elevation of  $[\text{Ca}^{2+}]_o$  was reversible and repeatable.

If the observed increase in  $[\text{Ca}^{2+}]_i$  occurred in the cytosol of the vascular smooth muscle cells rather than solely in endothelial cells or adventitial cells of the spiral modiolar artery, it would be expected that the increase in  $[\text{Ca}^{2+}]_o$  would cause the vessel to constrict. Therefore, in a second series of experiments, the effect of an elevation of  $[\text{Ca}^{2+}]_o$  on the vascular diameter was measured with videomicroscopy. Elevation of  $[\text{Ca}^{2+}]_o$  caused a biphasic vasoconstriction, which was reversible and repeatable (Fig. 1A and 2). The initial rate of this  $[\text{Ca}^{2+}]_o$ -induced vasoconstriction was  $2.01 \pm 0.06 \mu\text{m}/\text{sec}$  ( $n = 131$ ). The time course of this biphasic constriction paralleled the time course of the observed increase in  $[\text{Ca}^{2+}]_i$  suggesting that the increase in  $[\text{Ca}^{2+}]_i$  occurred in the cytosol of the vascular smooth muscle cells (Fig. 1). These findings are consistent with the hypothesis that the vascular smooth muscle cells of the spiral modiolar artery contain a CaSR.

The signal transduction mechanism linked to the CaSR is known to involve the release of  $\text{Ca}^{2+}$  from cytosolic stores. Cytosolic  $\text{Ca}^{2+}$  stores in vascular smooth muscle cells are known to slowly deplete in the presence of thapsigargin, which is an inhibitor of the endoplasmic reticulum  $\text{Ca}^{2+}$  ATPase (Treiman et al., 1998). If the  $[\text{Ca}^{2+}]_o$ -induced increase in  $[\text{Ca}^{2+}]_i$  would depend on release of  $\text{Ca}^{2+}$  from intracellular stores, it would be expected that depletion of these stores with thapsigargin would inhibit the  $[\text{Ca}^{2+}]_o$ -induced vasoconstriction. Therefore, in a third series of paired experiments, the effect of an elevation of  $[\text{Ca}^{2+}]_o$  on the vascular diameter was measured in the absence and presence of thapsigargin. Thapsigargin ( $10^{-9}$ – $10^{-6}$  M) caused a significant

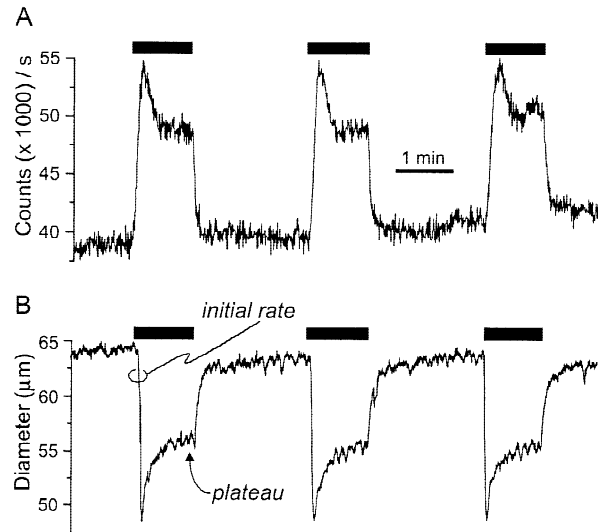


**Fig. 1.** Effect of an elevation of the  $[\text{Ca}^{2+}]_o$  on the  $[\text{Ca}^{2+}]_i$  and the vascular diameter of the spiral modiolar artery. (A) Elevation of  $[\text{Ca}^{2+}]_o$  from 1 to 10 mM (filled bars) caused a biphasic increase in  $[\text{Ca}^{2+}]_i$ , which was monitored as an increase in fluo-3 fluorescence intensity. (B) Elevation of  $[\text{Ca}^{2+}]_o$  from 1 to 10 mM (filled bars) caused a biphasic vasoconstriction. Note, that the increase in  $[\text{Ca}^{2+}]_i$  and the vasoconstriction were repeatable, reversible and similar in time course.

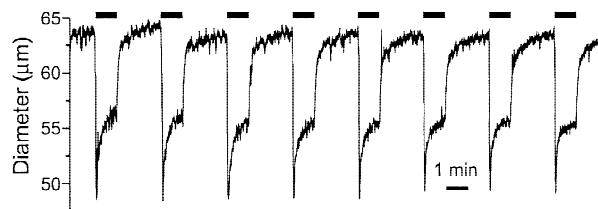


**Fig. 2.** Effect of an elevation of the  $[\text{Ca}^{2+}]_o$  on the vascular diameter of the spiral modiolar artery.  $[\text{Ca}^{2+}]_o$  was repeatedly elevated from 1 to 10 mM (filled bars). This experiment served as a control for experiments in which the  $[\text{Ca}^{2+}]_o$ -induced constriction was irreversibly inhibited, see Figs. 3 and 4.

concentration- and time-dependent attenuation of the initial rate but had no significant effect on the subsequent plateau (Fig. 3). Within 10 min, thapsigargin inhibited the initial rate of the  $[\text{Ca}^{2+}]_o$ -induced vasoconstriction with an  $\text{IC}_{50}$  of  $3 \times 10^{-9}$  M ( $n = 26$ ). This sensitivity to thapsigargin is consistent with a specific effect, namely depletion of the cytosolic  $\text{Ca}^{2+}$  stores, and thus provides evidence for the presence of CaSR in the smooth muscle cells of the spiral modiolar artery.

Further evidence for the involvement of  $\text{Ca}^{2+}$  stores in the  $[\text{Ca}^{2+}]_o$ -induced vasoconstriction can be obtained by interfering with  $\text{Ca}^{2+}$  release with ryanodine. Ryanodine has been shown to activate the ryanodine receptor calcium release channel in submicromolar concentrations (Jaggar et al., 2000; McPherson & Campbell, 1993). This stimulation of  $\text{Ca}^{2+}$  release empties the



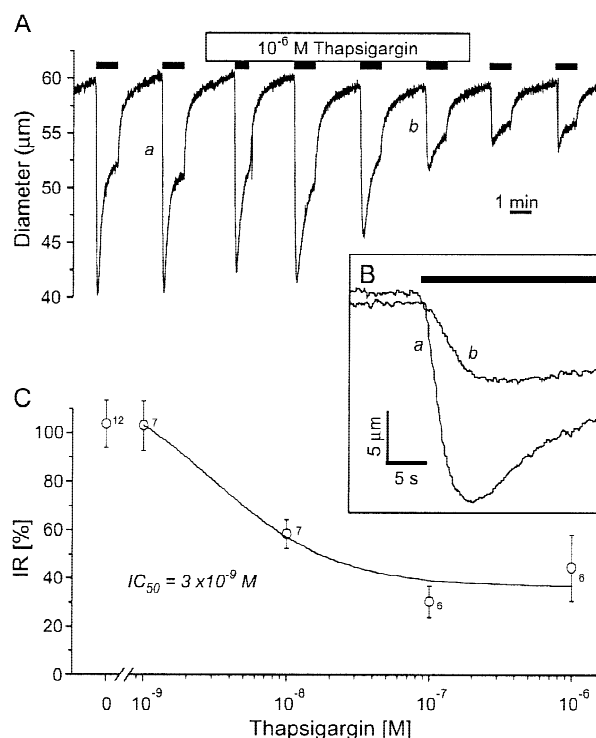


**Fig. 3.** Effect of thapsigargin on the  $[Ca^{2+}]_o$ -induced vasoconstriction. (A) Elevation of  $[Ca^{2+}]_o$  from 1 to 10 mM (filled bars) caused a biphasic vasoconstriction of the spiral modiolary artery that was inhibited by  $10^{-6}$  M thapsigargin. (B) Comparison of the time course of  $[Ca^{2+}]_o$ -induced vasoconstrictions in the absence (a) and in the presence (b) of  $10^{-6}$  M thapsigargin. Data are taken from A. Note that the initial rate in the presence of thapsigargin was significantly smaller. (C) Dose-response curve for the effect of thapsigargin on the initial rate (IR) of the  $[Ca^{2+}]_o$ -induced constriction. Data were normalized to the  $[Ca^{2+}]_o$ -induced constrictions in the beginning of the experiment, see A. The numbers next to the symbols depict the number of experiments.

stores and thereby may lead to an “virtual inhibition” of receptor-induced  $Ca^{2+}$  release from these stores. Therefore, in a fourth series of paired experiments, the effect of an elevation of  $[Ca^{2+}]_o$  on the vascular diameter was measured in the absence and presence of ryanodine. Ryanodine ( $10^{-9}$ – $10^{-6}$  M) caused a significant concentration- and time-dependent attenuation of the initial rate but had no significant effect on the subsequent plateau of the  $[Ca^{2+}]_o$ -induced vasoconstriction (Fig. 4). Within 10 min, ryanodine inhibited the initial rate of the  $[Ca^{2+}]_o$ -induced vasoconstriction with an  $IC_{50}$  of  $4 \times 10^{-8}$  M ( $n = 25$ ). This sensitivity to ryanodine is consistent with a specific effect on the cytosolic  $Ca^{2+}$ -stores and thus, provides evidence for the presence of a CaSR in the smooth muscle cells of the spiral modiolary artery. Further,  $10^{-6}$  M ryanodine causes a significant vasodilation from  $69 \pm 3$  to  $71 \pm 3$  μm ( $n = 6$ ). This vasodilation is an indicator that ryanodine indeed stimulated release of  $Ca^{2+}$  from the cytosolic stores (see Discussion).

CaSRs in tissues such as parathyroid gland, brain or

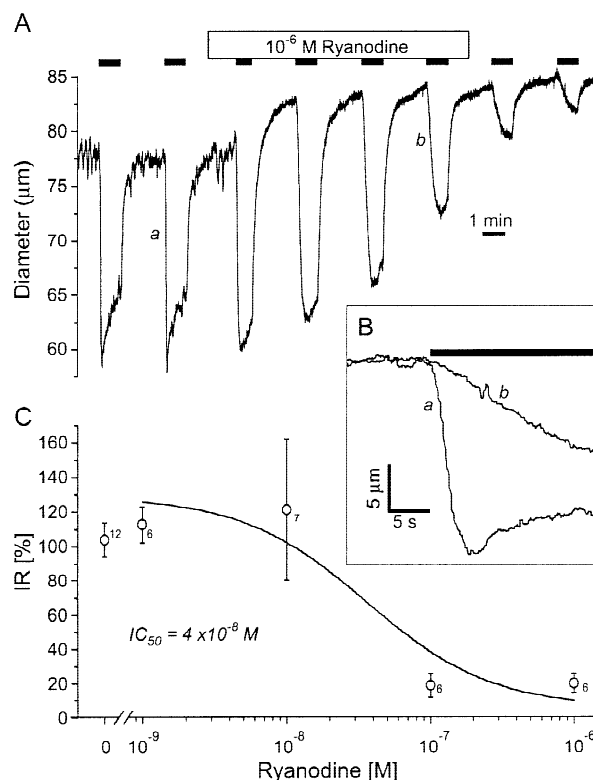


**Fig. 4.** Effect of ryanodine on the  $[Ca^{2+}]_o$ -induced vasoconstriction. (A) Elevation of  $[Ca^{2+}]_o$  from 1 to 10 mM (filled bars) caused a biphasic vasoconstriction of the spiral modiolary artery that was inhibited by  $10^{-6}$  M ryanodine. Note that  $10^{-6}$  M ryanodine caused a vasodilation consistent with release of  $Ca^{2+}$  from ryanodine-sensitive stores (see Discussion). (B) Comparison of the time course of  $[Ca^{2+}]_o$ -induced vasoconstrictions in the absence (a) and in the presence (b) of  $10^{-6}$  M ryanodine. Data are taken from A. Note that the initial rate in the presence of ryanodine was significantly smaller. (C) Dose-response curve for the effect of ryanodine on the initial rate (IR) of the  $[Ca^{2+}]_o$ -induced constriction. Data were normalized to the  $[Ca^{2+}]_o$ -induced constrictions in the beginning of the experiment, see A. The numbers next to the symbols depict the number of experiments.

ovarian surface epithelial cells have been shown to signal via PLC (Brown et al., 1993; Ruat et al., 1996; McNeil et al., 1998). If PLC is part of the signaling pathway mediating  $[Ca^{2+}]_o$ -induced vasoconstriction in the spiral modiolary artery, it would be expected that the  $[Ca^{2+}]_o$ -induced constriction will be sensitive to inhibitors of PLC. Thus, in a fifth series of paired experiments, the effect of the PLC-inhibitor U73122 and its inactive analogue U73343 on  $[Ca^{2+}]_o$ -induced constriction was determined. Within 7 min  $10^{-6}$  M U73122 reduced the initial rate of the  $[Ca^{2+}]_o$ -induced vasoconstriction to  $45 \pm 10\%$  ( $n = 8$ ) whereas the inactive analogue U73343 had no significant effect ( $95 \pm 15\%$ ,  $n = 6$ , Fig. 5). These observations are consistent with the hypothesis that the spiral modiolary artery contains a CaSR and that this receptor signals via the PLC pathway.

Polyvalent cations such as  $Ca^{2+}$ ,  $Mg^{2+}$ ,  $Gd^{3+}$ ,  $Ni^{2+}$

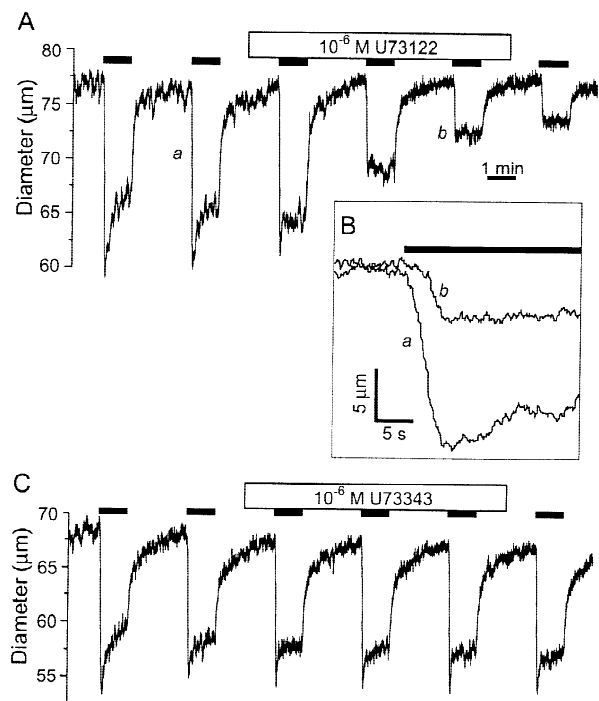


**Fig. 5.** Effect of U73122 and U73343 on the  $[Ca^{2+}]_o$ -induced vasoconstriction. (A) Elevation of  $[Ca^{2+}]_o$  from 1 to 10 mM (filled bars) caused a biphasic vasoconstriction of the spiral modiolar artery that was inhibited by  $10^{-6}$  M U73122. (B) Comparison of the time course of  $[Ca^{2+}]_o$ -induced vasoconstrictions in the absence (a) and in the presence (b) of  $10^{-6}$  M U73122. Data are taken from A. (C) The inactive analogue  $10^{-6}$  M U73343 had no significant effect on  $[Ca^{2+}]_o$ -induced vasoconstrictions.

and neomycin have been shown to be agonists for CaSRs. For the first three ions there is a common rank potency order of  $Gd^{3+} > Ca^{2+} > Mg^{2+}$  (Nemeth & Scarpa, 1987; Brown et al., 1993; Riccardi et al., 1995; Ruat et al., 1996; McGehee et al., 1997). If  $Mg^{2+}$ ,  $Gd^{3+}$ ,  $Ni^{2+}$  or neomycin were agonists for the CaSR in the spiral modiolar artery, it would be expected that these polyvalent cations would cause a vasoconstriction similar to that observed in response to an elevation in the  $[Ca^{2+}]_o$ . Therefore, in a sixth series of experiments, polyvalent cations were tested for agonist potency in the presence of 1 mM  $Ca^{2+}$ .  $Ca^{2+}$ ,  $Gd^{3+}$  and  $Ni^{2+}$  caused a concentration-dependent vasoconstriction, whereas  $Mg^{2+}$  and neomycin did not have an effect on the vascular diameter (Fig. 6). The rank potency order was  $Gd^{3+} > Ni^{2+} > Ca^{2+} \gg$  neomycin =  $Mg^{2+}$ . This rank potency order is consistent with that commonly found for CaSRs although neomycin has been shown to be an agonist in CaSRs of other tissues (Brown et al., 1993; Riccardi et al., 1995).

If the  $[Ca^{2+}]_o$ -induced constriction of the spiral modiolar artery is mediated by the CaSR rather than by voltage-sensitive L-type  $Ca^{2+}$  channels, it would be ex-

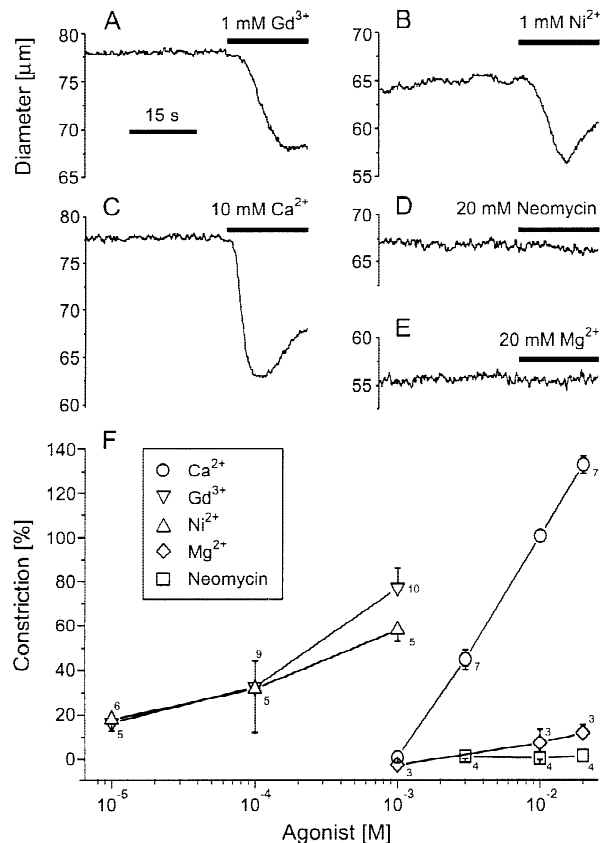


**Fig. 6.** Effect of polyvalent cations on the vascular diameter of the spiral modiolar artery. (A–E)  $Gd^{3+}$ ,  $Ni^{2+}$  and  $Ca^{2+}$  caused a biphasic constriction of the spiral modiolar artery, whereas neomycin and  $Mg^{2+}$  did not. The axis label and time bar shown in A pertain to A–E. (F) Dose-response curves for the effects of  $Gd^{3+}$ ,  $Ni^{2+}$ ,  $Ca^{2+}$ , neomycin and  $Mg^{2+}$  on the vascular diameter of the spiral modiolar artery. Data were normalized to constrictions induced by an elevation from 1 to 10 mM  $Ca^{2+}$ , which were performed in the beginning of each experiment. The numbers next to the symbols depict the number of experiments.

pected that this response will be insensitive to inhibitors of L-type  $Ca^{2+}$  channels. Thus, in a seventh series of paired experiments, the effect of the L-type  $Ca^{2+}$  channel blocker nifedipine on the  $[Ca^{2+}]_o$ -induced vasoconstriction was determined. Nifedipine ( $10^{-6}$  M) had no significant effect on the initial rate of the  $[Ca^{2+}]_o$ -induced vasoconstriction ( $93.2 \pm 7.9\%$ ,  $n = 4$ , Fig. 7). The effectiveness of nifedipine to inhibit L-type  $Ca^{2+}$  channels was verified in each experiment by pairing it with a positive control. Nifedipine at a concentration of  $10^{-6}$  M was expected to fully inhibit  $K^+$ -induced vasoconstrictions since the  $IC_{50}$  for nifedipine in the spiral modiolar artery is known to be  $2 \times 10^{-9}$  M (Wangemann et al., 1998). A significant inhibition of  $K^+$ -induced vasoconstriction by  $10^{-6}$  M nifedipine was taken here as evidence for the effectiveness of the drug. Taken together, these observations demonstrate that L-type  $Ca^{2+}$  channels are not involved in  $[Ca^{2+}]_o$ -induced vasoconstriction of the

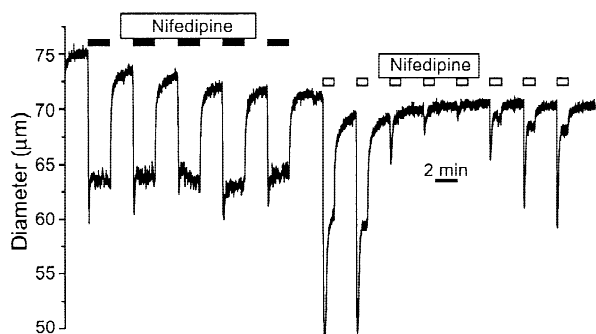


**Fig. 7.** Effect of nifedipine on  $[\text{Ca}^{2+}]_o$ -induced and  $\text{K}^+$ -induced vasoconstriction. Elevation of  $[\text{Ca}^{2+}]_o$  from 1 to 10 mM (filled bars) caused a vasoconstriction of the spiral modiolary artery that was insensitive to  $10^{-6}$  M nifedipine. Elevation of the  $\text{K}^+$ -concentration from 3.6 to 150 mM (open bars) caused a transient vasoconstriction that was significantly inhibited by  $10^{-6}$  M nifedipine.

spiral modiolary artery. Thus, this finding is consistent with the view that the  $[\text{Ca}^{2+}]_o$ -induced vasoconstriction is mediated by the CaSR.

$\text{Gd}^{3+}$  is not only an agonist of the CaSR but also an inhibitor of ion channels including T-type  $\text{Ca}^{2+}$  channels. If  $[\text{Ca}^{2+}]_o$ -induced constriction of the spiral modiolary artery is mediated by the CaSR rather than by  $\text{Ca}^{2+}$  influx through T-type  $\text{Ca}^{2+}$  channels, it would be expected that  $[\text{Ca}^{2+}]_o$ -induced constriction will be insensitive to micromolar concentrations of  $\text{Gd}^{3+}$ . Indeed,  $\text{Gd}^{3+}$  is known to block T-type  $\text{Ca}^{2+}$  channels with an  $\text{IC}_{50}$  of  $3 \times 10^{-7}$  M (Mlinar & Enyeart, 1993). Thus, in an eighth series of paired experiments, the effect of the nonspecific blocker  $\text{Gd}^{3+}$  on the  $[\text{Ca}^{2+}]_o$ -induced vasoconstriction was determined.  $\text{Gd}^{3+}$  inhibited the initial rate of the  $[\text{Ca}^{2+}]_o$ -induced vasoconstriction with an  $\text{IC}_{50}$  of  $(7 \pm 3) \times 10^{-5}$  M ( $n = 34$ , Fig. 8). Neither  $10^{-7}$  M nor  $10^{-6}$  M  $\text{Gd}^{3+}$  had a significant effect. These observations are consistent with the view that the  $[\text{Ca}^{2+}]_o$ -induced vasoconstriction is mediated by the CaSR rather than by a  $\text{Ca}^{2+}$  influx via  $\text{Gd}^{3+}$ -sensitive T-type  $\text{Ca}^{2+}$  channels. The rather high  $\text{IC}_{50}$  for  $\text{Gd}^{3+}$  on  $[\text{Ca}^{2+}]_o$ -induced vasoconstriction is consistent with a nonspecific effect. Indeed, high concentrations of  $\text{Gd}^{3+}$  have been shown to inhibit capacitative- $\text{Ca}^{2+}$ -influx mechanisms, a  $\text{Ca}^{2+}$ -ATPase of the sarcoplasmic reticulum and  $\text{IP}_3$ -formation (Imamura & Kawakita, 1991; Wenzel-Seifert et al., 1996; Mailland et al., 1997; Broad et al., 1999).

Further,  $\text{Ni}^{2+}$  is not only an agonist of the CaSR but also an inhibitor of  $\text{Na}^+/\text{Ca}^{2+}$  exchangers. If  $[\text{Ca}^{2+}]_o$ -induced vasoconstriction of the spiral modiolary artery is mediated by the CaSR rather than by  $\text{Ca}^{2+}$  influx through a  $\text{Na}^+/\text{Ca}^{2+}$  exchanger operating in the reverse mode, it would be expected that  $[\text{Ca}^{2+}]_o$ -induced constriction will be insensitive to  $10^{-4}$  M  $\text{Ni}^{2+}$ . Indeed,  $\text{Ni}^{2+}$  is known to block  $\text{Na}^+/\text{Ca}^{2+}$  exchangers with an  $\text{IC}_{50}$  between  $5 \times 10^{-4}$  M and  $5 \times 10^{-5}$  M (Iwamoto & Shigekawa, 1998). Thus,

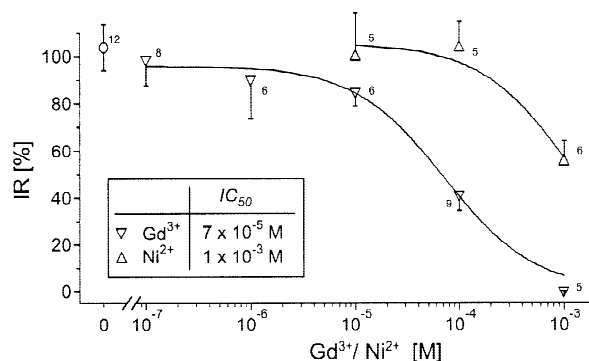


**Fig. 8.** Dose-response curves for the effect of  $\text{Gd}^{3+}$  and  $\text{Ni}^{2+}$  on the initial rate (IR) of the  $[\text{Ca}^{2+}]_o$ -induced vasoconstriction. Data were normalized to the  $[\text{Ca}^{2+}]_o$ -induced constrictions in the beginning of the experiment. The numbers next to the symbols depict the number of experiments.

in a ninth series of paired experiments, the effect of  $\text{Ni}^{2+}$  on  $[\text{Ca}^{2+}]_o$ -induced vasoconstriction was determined.  $\text{Ni}^{2+}$  blocked  $[\text{Ca}^{2+}]_o$ -induced vasoconstriction with an  $\text{IC}_{50}$  of  $(1 \pm 1) \times 10^{-3}$  M ( $n = 16$ , Fig. 8). Neither  $10^{-5}$  M nor  $10^{-4}$  M  $\text{Ni}^{2+}$  had a significant effect. These observations are consistent with the view that the  $[\text{Ca}^{2+}]_o$ -induced vasoconstriction is mediated by the CaSR rather than by a  $\text{Ca}^{2+}$  influx via a  $\text{Na}^+/\text{Ca}^{2+}$  exchanger. The rather high  $\text{IC}_{50}$  of  $\text{Ni}^{2+}$  on  $[\text{Ca}^{2+}]_o$ -induced constriction is most likely due to a nonspecific effect.

In addition to the functional evidence for the presence of a CaSR in the spiral modiolary artery, the presence of CaSR transcripts was determined by RT-PCR. In a tenth series of experiments RT-PCR was performed on total RNA extracted from the spiral modiolary artery with primer pairs specific for CaSR transcripts. Reactions revealed RT-PCR products of the expected size of 448 bp (Fig. 9, lane marked 'SMA +'). This observation suggests that the spiral modiolary artery contains transcripts for a CaSR. The specificity of the CaSR primers was verified through RT-PCR performed with total RNA extracted from gerbil kidney (Fig. 9, lane marked 'Kidney +'), which is known to contain a CaSR. Total RNA extracted from gerbil blood was tested for the presence of CaSR transcripts. No RT-PCR product was found verifying that blood remaining in the isolated spiral modiolary artery did not provide a source of message for CaSRs. This observation suggests that the CaSR is located in the arteriolar wall. The identity of PCR products resulting from RT-PCR reactions performed with total RNA extracted from gerbil kidney and spiral modiolary artery was confirmed by sequencing the products and comparing the sequences to known sequences (Table). The nucleotide sequences of the amplified fragments of the CaSR from the gerbil spiral modiolary artery has been deposited in GenBank under the accession number AF221064. The sequence given excludes the primer sequences.

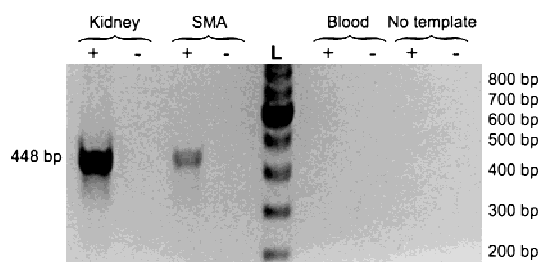


**Fig. 9.** Agarose gel electrophoresis of reverse-transcriptase polymerase chain reaction (RT-PCR) products. RT-PCR was performed with gene-specific primers for the CaSR on 0.1  $\mu$ g of total RNA obtained from the kidney, 1.0  $\mu$ g of total RNA obtained from the spiral modiolary artery and 0.5  $\mu$ g of total RNA obtained from blood in the presence (+) or absence (-) of reverse transcriptase. The DNA markers (L) consisted of 15 blunt-ended fragments between 100 and 1500 bp in multiples of 100 bp (*not all are shown*). Note that a band of the expected size was found in the kidney and the spiral modiolary artery but not in blood. The observation that no product of the expected size was obtained from blood rules out the possibility that blood, which was a containment of the microdissected spiral modiolary arteries, provided a source for transcripts for the CaSR. The observation that no products were observed when reactions were performed in the absence of reverse transcriptase (-) or in the absence of templates (*no template*) demonstrates that RNA samples were free of contamination.

**Table** Accession # and % identity of sequenced PCR products

	Gerbil kidney and spiral modiolary artery #AF221064
Rat CaSR	90% in 411 bp
#U20289	95% in 137 aa
Murine CaSR	91% in 411 bp
#AF110179	94% in 137 aa
Bovine CaSR	92% in 411 bp
#S67307	96% in 137 aa
Human	90% in 411 bp
#NM000388	96% in 137 aa

## Discussion

Several lines of evidence support the conclusion that the spiral modiolary artery senses  $[\text{Ca}^{2+}]_o$  via a CaSR. First, an elevation of  $[\text{Ca}^{2+}]_o$  caused a biphasic increase in  $[\text{Ca}^{2+}]_i$ , which is likely to be localized in the vascular smooth muscle cells of the spiral modiolary artery, since it was paralleled by a biphasic vasoconstriction. Second, the initial phase of the  $[\text{Ca}^{2+}]_o$ -induced constriction was dependent on  $\text{Ca}^{2+}$ -release from thapsigargin- and ryanodine-sensitive intracellular stores. Figure 10 summarizes our hypothesis regarding the interaction of the CaSR with the cytosolic  $\text{Ca}^{2+}$  stores. Third, the initial phase of the  $[\text{Ca}^{2+}]_o$ -induced constriction was sensitive to U73122, suggesting that  $[\text{Ca}^{2+}]_o$ -induced constriction was dependent on PLC-activation. Fourth, the CaSR-

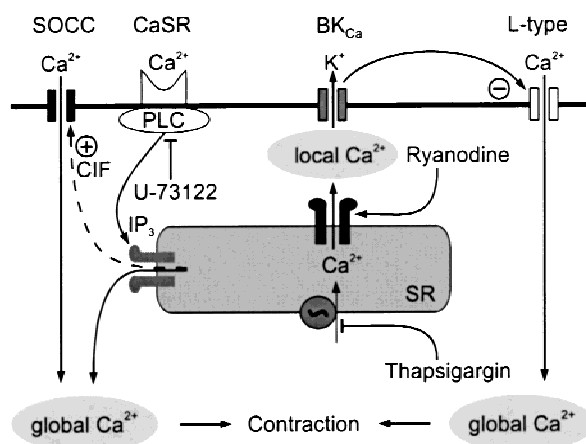


**Fig. 10.** Proposed signal transduction mechanism of the CaSR in the spiral modiolary artery. Extracellular  $\text{Ca}^{2+}$  is an agonist at the CaSR. The CaSR activates PLC and releases  $\text{Ca}^{2+}$  via  $\text{IP}_3$  from the sarcoplasmic reticulum (SR) leading to an increase in the global cytosolic  $\text{Ca}^{2+}$  concentration and a contraction. A further increase in the global cytosolic  $\text{Ca}^{2+}$  concentration may result from  $\text{Ca}^{2+}$  influx via store-operated  $\text{Ca}^{2+}$  channels (SOCC) in the plasma membrane, which may be activated via a putative calcium influx factor (CIF). Release of  $\text{Ca}^{2+}$  from the sarcoplasmic reticulum can be reduced by thapsigargin, which inhibits the  $\text{Ca}^{2+}$  ATPase and by submicromolar ryanodine concentrations, which empty the sarcoplasmic reticulum by stimulating  $\text{Ca}^{2+}$  release. The ryanodine-induced local increase in the cytosolic  $\text{Ca}^{2+}$  concentration activates  $\text{Ca}^{2+}$ -sensitive  $\text{K}^+$  channels ( $\text{BK}_{\text{Ca}}$ ). Activation of these  $\text{K}^+$  channels hyperpolarizes the membrane potential leading to an inactivation of L-type  $\text{Ca}^{2+}$  channels, a decrease in the global cytosolic  $\text{Ca}^{2+}$  concentration and a vasodilation.

agonists  $\text{Gd}^{3+}$  and  $\text{Ni}^{2+}$  caused a biphasic dose-dependent constriction of the spiral modiolary artery, which was similar to that observed in response to an elevation of  $[\text{Ca}^{2+}]_o$ . Fifth, the vascular wall of the spiral modiolary artery contained transcripts for the CaSR. Similar observations have been made in other tissues known to contain a CaSR (Brown et al., 1993; Riccardi et al., 1995; Ruat et al., 1996; McGehee et al., 1997; Adebajo et al., 1998; McNeil et al., 1998).

The agonist rank potency order for the CaSR in the spiral modiolary artery was  $\text{Gd}^{3+} > \text{Ni}^{2+} > \text{Ca}^{2+} \gg \text{Mg}^{2+} = \text{neomycin}$ . Most CaSRs are characterized by a rank potency of  $\text{Gd}^{3+} > \text{Ca}^{2+} > \text{Mg}^{2+}$  although variations in potency orders have been found. For example,  $\text{Mg}^{2+}$  has been shown to be an agonist for the CaSR of bovine parathyroid and rat kidney (Riccardi et al., 1995; McNeil et al., 1998) but not for the CaSR of sheep parafollicular cells and murine Leydig-cells (McGehee et al., 1997; Adebajo et al., 1998). Similar variations have been found for neomycin that has been shown to be an agonist for bovine parathyroid and rat kidney CaSRs but not for rabbit thick ascending limb CaSR (Brown et al., 1993; Desfleurs et al., 1999). This heterogeneity in the agonist rank potency order might be related to species-specific



differences among CaSRs. Further,  $\text{Ni}^{2+}$  was a more potent agonist than  $\text{Ca}^{2+}$  for the spiral modiolar artery CaSR. A similar potency order has been observed for the CaSR in murine Leydig cells (Adebanjo et al., 1998).

In most tissues CaSRs have been found to be linked to a phosphatidylinositol-specific PLC (Brown et al., 1993; Ruat et al., 1996; McNeil et al., 1998). This PLC is known to be sensitive to U73122 (Smith et al., 1990; Yule & Williams, 1992). In contrast, CaSRs in sheep thyroid parafollicular cells have been shown to be linked to an U73122-insensitive phosphatidylcholine-specific PLC (McGehee et al., 1997). The observation that U73122 inhibited  $[\text{Ca}^{2+}]_o$ -induced constriction of the spiral modiolar artery suggests that the CaSR of the spiral modiolar artery is linked to a phosphatidylinositol-specific PLC.

The observation that  $10^{-6}$  M ryanodine caused a significant vasodilation is of great interest (Fig. 4). As shown by Nagasaki and Fleischer (1988) and most recently reviewed by Jaggar et al. (2000), ryanodine at these concentrations stimulates  $\text{Ca}^{2+}$  release from the sarcoplasmic reticulum. This stimulation of  $\text{Ca}^{2+}$  release may have caused an increase in the local cytosolic  $\text{Ca}^{2+}$  concentration in the subplasmalemmal space rather than an increase in the global cytosolic  $\text{Ca}^{2+}$  concentration surrounding the contractile filaments. As illustrated in Fig. 10, it is conceivable, that ryanodine-induced  $\text{Ca}^{2+}$  release raises the local  $\text{Ca}^{2+}$  concentration near  $\text{Ca}^{2+}$ -dependent  $\text{K}^+$  channels (Perez et al., 1999; Jaggar et al., 2000). Activation of the  $\text{Ca}^{2+}$ -dependent  $\text{K}^+$  channels would cause a hyperpolarization, closing of L-type  $\text{Ca}^{2+}$  channels resulting in a decrease in the global  $\text{Ca}^{2+}$  concentration and a vasodilation (Nelson et al., 1995). Support for this hypothesis comes from the observations that  $10^{-6}$  M ryanodine caused a significant dilation of the spiral modiolar artery (see Fig. 4) and that  $10^{-9}$  M nifedipine, a L-type  $\text{Ca}^{2+}$  channel blocker, causes a vasodilation of the spiral modiolar artery (Wangemann et al., 1998).

The CaSR of the spiral modiolar artery is likely to be localized in the vascular smooth muscle cells of the arteriolar wall rather than in endothelial cells, adventitial cells or perivascular nerves. Evidence for a localization in the smooth muscle cells comes from the finding that the  $[\text{Ca}^{2+}]_o$ -induced increase in  $[\text{Ca}^{2+}]_i$  occurred with the same time course as the  $[\text{Ca}^{2+}]_o$ -induced vasoconstriction (Fig. 1). A localization in endothelial cells or adventitial cells cannot be ruled out although a far more complex interaction between these cells and the vascular smooth muscle cells would need to be proposed. Further, a localization in perivascular nerves as observed in mesentery resistance arteries (Bukoski et al., 1997) is unlikely, since CaSR transcripts were found in the spiral modiolar artery. In contrast, mesentery resistance arteries, which contain CaSR-proteins, yielded no CaSR-

transcripts, since the presence of transcripts is generally restricted to the nerve cell bodies located in remote ganglia.

Most physiologic relevant receptors face changes in the agonist concentration. Thus, the question regarding the physiologic relevance of the CaSR in the spiral modiolar artery is linked to the question whether or not this receptor faces variations in the  $[\text{Ca}^{2+}]_o$ . Variations in the  $[\text{Ca}^{2+}]_o$  in the vicinity of the spiral modiolar artery are conceivable since this arteriole is sandwiched between the eighth cranial nerve and the bone of the cochlear modiolus. The  $[\text{Ca}^{2+}]_o$  in the direct vicinity of bone-osteoclasts has been shown to be as high as 40 mM (Silver et al., 1988). The CaSR could allow the spiral modiolar artery to sense the  $[\text{Ca}^{2+}]_o$ , which could regulate the vascular diameter of this arteriole. The physiologic relevance of this regulatory mechanism, however, remains unclear.

Alternatively, it is conceivable, that the  $[\text{Ca}^{2+}]_o$  is an indicator to the spiral modiolar artery of its proximity to the cochlear bone. Sensing and responding to an elevated  $[\text{Ca}^{2+}]_o$  might protect the spiral modiolar artery from being overgrown by the cochlea bone. Control of bone formation could be mediated by paracrine secretion of chemicals interfering with bone growth. In the context of this hypothesis, the observed  $[\text{Ca}^{2+}]_o$ -induced constriction of the spiral modiolar artery could merely be an epiphenomenon, which allowed the demonstration of the CaSR, rather than an indication that the  $[\text{Ca}^{2+}]_o$  regulates the vascular diameter via this receptor. This hypothesis remains to be tested and may possibly be extended to other blood vessels, which are enclosed by bone without being overgrown.

In conclusion, the present study demonstrates that the spiral modiolar artery contains a CaSR, which is most likely located in the vascular smooth muscle cells. If so, the present study may be the first demonstration of a CaSR in vascular smooth muscle cells.

The support by Research Grant RO1-DC04280 from the National Institute on Deafness and Other Communication Disorders, National Institutes of Health is gratefully acknowledged.

## References

- Adebanjo, O.A., Igietseme, J., Huang, C.L., Zaidi, M. 1998. The effect of extracellularly applied divalent cations on cytosolic  $\text{Ca}^{2+}$  in murine leydig cells: evidence for a  $\text{Ca}^{2+}$ -sensing receptor. *J. Physiol.* **513**:399–410
- Altura, B.T., Altura, B.M. 1978. Factors Affecting Vascular Responsiveness. (Chapter 14). B.M. Altura and B. Kaley editors. pp. 547–615. University Park Press, Baltimore
- Berridge, M.J. 1993. Inositol trisphosphate and calcium signaling. *Nature* **361**:315–325
- Broad, L.M., Cannon, T.R., Taylor, C.W. 1999. A non-capacitative pathway activated by arachidonic acid is the major  $\text{Ca}^{2+}$  entry

- mechanism in rat A7r5 smooth muscle cells stimulated with low concentrations of vasopressin. *J. Physiol.* **517**:121–134
- Brown, E.M., Gamba, G., Riccardi, D., Lombardi, M., Butters, R., Kifor, O., Sun, A., Hediger, M.A., Lytton, J., Hebert, S.C. 1993. Cloning and characterization of an extracellular  $\text{Ca}^{2+}$ -sensing receptor from bovine parathyroid. *Nature* **366**:575–580
- Bukoski, R.D., Bian, K., Wang, Y., Mupanomunda, M. 1997. Perivascular sensory nerve  $\text{Ca}^{2+}$  receptor and  $\text{Ca}^{2+}$ -induced relaxation of isolated arteries. *Hypertension* **30**:1431–1439
- Chattopadhyay, N., Ye, C., Singh, D.P., Kifor, O., Vassilev, P.M., Shinohara, T., Chylack, L.T.J., Brown, E.M. 1997. Expression of extracellular calcium-sensing receptor by human lens epithelial cells. *Biochem. Biophys. Res. Commun.* **233**:801–805
- Desfleurs, E., Wittner, M., Pajaud, S., Nitschke, R., Rajerison, R.M., Di Stefano, A. 1999. The  $\text{Ca}^{2+}$ -sensing receptor in the rabbit cortical thick ascending limb (cTAL) is functionally not coupled to phospholipase C. *Pfluegers Arch.* **437**:716–723
- Imamura, Y., Kawakita, M. 1991. Analysis of the binding sites of  $\text{Gd}^{3+}$  on  $\text{Ca}^{2+}$ -transporting ATPase of the sarcoplasmic reticulum through its effects on fluorescence of tryptophan residues and a covalently attached fluorescent probe N-(1-anilino-naphthyl-4)-maleimide. *J. Biochem.* **110**:214–219
- Ito, K., Ikemoto, T., Takakura, S. 1991. Involvement of  $\text{Ca}^{2+}$  influx-induced  $\text{Ca}^{2+}$  release in contractions of intact vascular smooth muscles. *Am. J. Physiol.* **261**:H1464–H1470
- Iwamoto, T., Shigekawa, M. 1998. Differential inhibition of  $\text{Na}^+/\text{Ca}^{2+}$  exchanger isoforms by divalent cations and isothiourea derivative. *Am. J. Physiol.* **275**:C423–C430
- Jagger, J.H., Porter, V.A., Lederer, W.J., Nelson, M.T. 2000. Calcium sparks in smooth muscle. *Am. J. Physiol.* **278**:C235–C256
- Mailland, M., Waelchli, R., Ruat, M., Boddeke, H.G., Seuwen, K. 1997. Stimulation of cell proliferation by calcium and a calcimimetic compound. *Endocrinology* **138**:3601–3605
- McGehee, D.S., Aldersberg, M., Liu, K.P., Hsuang, S., Heath, M.J., Tamir, H. 1997. Mechanism of extracellular  $\text{Ca}^{2+}$  receptor-stimulated hormone release from sheep thyroid parafollicular cells. *J. Physiol.* **502**:31–44
- McNeil, L., Hobson, S., Nipper, V., Rodland, K.D. 1998. Functional calcium-sensing receptor expression in ovarian surface epithelial cells. *Am. J. Obstet. Gynecol.* **178**:305–313
- McPherson, P.S., Campbell, K.P. 1993. The ryanodine receptor/ $\text{Ca}^{2+}$  release channel. *J. Biol. Chem.* **268**:13765–13768
- Mlinar, B., Enyeart, J.J. 1993. Block of current through T-type calcium channels by trivalent metal cations and nickel in neural rat and human cells. *J. Physiol.* **469**:639–652
- Morgan, K.G. 1987. Calcium and vascular smooth muscle tone. *Am. J. Med.* **82**:9–15
- Nagasaki, K., Fleischer, S. 1988. Ryanodine sensitivity of the calcium release channel of sarcoplasmic reticulum. *Cell Calcium* **9**:1–7
- Nelson, M.T., Cheng, H., Rubart, M., Santana, L.F., Bonev, A.D., Knot, H.J., Lederer, W.J. 1995. Relaxation of arterial smooth muscle by calcium sparks. *Science* **270**:633–637
- Nemeth, E.F. 1995.  $\text{Ca}^{2+}$  Receptor-dependent Regulation of Cellular Functions. *NIPS* **10**:1–5
- Nemeth, E.F., Scarpa, A. 1987. Rapid mobilization of cellular  $\text{Ca}^{2+}$  in bovine parathyroid cells evoked by extracellular divalent cations. Evidence for a cell surface calcium receptor. *J. Biol. Chem.* **262**:5188–5196
- Noguera, M.A., Madrero, Y., Ivorra, M.D., D'Ocon, P. 1998. Characterization of two different  $\text{Ca}^{2+}$  entry pathways dependent on depletion of internal  $\text{Ca}^{2+}$  pools in rat aorta. *Naunyn Schmiedeberg Arch. Pharmacol.* **357**:92–99
- Perez, G.J., Bonev, A.D., Patlak, J.B., Nelson, M.T. 1999. Functional coupling of ryanodine receptors to  $\text{K}_{\text{Ca}}$  channels in smooth muscle cells from rat cerebral arteries. *J. Gen. Physiol.* **113**:229–238
- Putney, J.W.J., McKay, R.R. 1999. Capacitative calcium entry channels. *Bioessays* **21**:38–46
- Riccardi, D., Park, J., Lee, W.S., Gamba, G., Brown, E.M., Hebert, S.C. 1995. Cloning and functional expression of a rat kidney extracellular calcium/polyvalent cation-sensing receptor. *Proc. Natl. Acad. Sci. USA* **92**:131–135
- Ruat, M., Molliver, M.E., Snowman, A.M., Snyder, S.H. 1995. Calcium sensing receptor: molecular cloning in rat and localization to nerve terminals. *Proc. Natl. Acad. Sci. USA* **92**:3161–3165
- Ruat, M., Snowman, A.M., Hester, L.D., Snyder, S.H. 1996. Cloned and expressed rat  $\text{Ca}^{2+}$ -sensing receptor. *J. Biol. Chem.* **271**:5972–5975
- Silver, I.A., Murrills, R.J., Etherington, D.J. 1988. Microelectrode studies on the acid microenvironment beneath adherent macrophages and osteoclasts. *Exp. Cell Res.* **175**:266–276
- Smith, R.J., Sam, L.M., Justen, J.M., Bundy, G.L., Bala, G.A., Bleasdale, J.E. 1990. Receptor-coupled signal transduction in human polymorphonuclear neutrophils: effects of a novel inhibitor of phospholipase C-dependent processes on cell responsiveness. *J. Pharmacol. Exp. Ther.* **253**:688–697
- Treiman, M., Caspersen, C., Christensen, S.B. 1998. A tool coming of age: thapsigargin as an inhibitor of sarco-endoplasmic reticulum  $\text{Ca}^{2+}$ -ATPases. *Trends. Pharmacol. Sci.* **19**:131–135
- Uchida, E., Bohr, D.F. 1969. Myogenic tone in isolated perfused resistance vessels from rats. *Am. J. Physiol.* **216**:1343–1350
- Wangemann, P., Cohn, E.S., Gruber, D.D., Gratton, M.A. 1998.  $\text{Ca}^{2+}$ -dependence and nifedipine-sensitivity of vascular tone and contractility in the isolated superfused spiral modiolar artery in vitro. *Hear. Res.* **118**:90–100
- Wangemann, P., Gruber, D.D. 1998. The isolated in vitro perfused spiral modiolar artery: pressure dependence of vasoconstriction. *Hear. Res.* **115**:113–118
- Webb, R.C., Bohr, D.F. 1978. Mechanism of membrane stabilization by calcium in vascular smooth muscle. *Am. J. Physiol.* **235**:C227–C232
- Wenzel-Seifert, K., Krautwurst, D., Musgrave, I., Seifert, R. 1996. Thapsigargin activates univalent- and bivalent-cation entry in human neutrophils by a SK&F I3 96365- and  $\text{Gd}^{3+}$ -sensitive pathway and is a partial secretagogue: involvement of pertussis-toxin-sensitive G- proteins and protein phosphatases 1/2A and 2B in the signal-transduction pathway. *Biochem. J.* **314**:679–686
- Wonneberger, K., Scofield, M.A., Wangemann, P. 2000.  $\text{Ca}^{2+}$ -induced contractions of the spiral modiolar artery are mediated by a  $\text{Ca}^{2+}$ -sensing receptor (CaR): functional and molecular biologic evidence. *Assoc. Res. Otolaryngol.* **23**:225
- Wonneberger, K., Wangemann, P. 1999. The vascular tone of the spiral modiolar artery is sensitive to changes in the extravascular  $\text{Ca}^{2+}$  but not  $\text{Mg}^{2+}$  concentration. *Assoc. Res. Otolaryngol.* **22**:821
- Wylam, M.E., Samsel, R.W., Schumacker, P.T., Umans, J.G. 1993. Extracellular calcium and intrinsic tone in the human umbilical artery. *J. Pharmacol. Exp. Ther.* **266**:1475–1481
- Yule, D.I., Williams, J.A. 1992. U73122 inhibits  $\text{Ca}^{2+}$  oscillations in response to cholecystokinin and carbachol but not to JMV-180 in rat pancreatic acinar cells. *J. Biol. Chem.* **267**:13830–13835
- Zaidi, M., Alam, A.S., Huang, C.L., Pazianas, M., Bax, C.M., Bax, B.E., Moonga, B.S., Bevis, P.J., Shankar, V.S. 1993. Extracellular  $\text{Ca}^{2+}$  sensing by the osteoclast. *Cell Calcium* **14**:271–277